Effect of membrane stiffness and cytoskeletal element density on mechanical stimuli within cells: an analysis of the consequences of ageing in cells

Published in:
Computer Methods in Biomechanics and Biomedical Engineering

Document Version:
Peer reviewed version

Effect of membrane stiffness and cytoskeletal element density on mechanical stimuli within cells: an analysis of the consequences of ageing in cells

Feng Xue[a], Alex B. Lennon[a], Katey K. McKayed[a, b], Veronica A. Campbell[a, b] and Patrick J. Prendergast[a]

[a] Trinity Centre for Bioengineering, School of Engineering, Trinity College Dublin, Ireland

[b] Department of Physiology, School of Medicine, Trinity College Dublin, Ireland

Correspondence to Patrick J Prendergast, Ph.D., Sc.D.

Email: pprender@tcd.ie

Abstract

A finite element model of a single cell was created and used to compute the biophysical stimuli generated within a cell under mechanical loading. Major cellular components were incorporated in the model: the membrane, cytoplasm, nucleus, microtubules, actin filaments, intermediate filaments, nuclear lamina and chromatin. The model used multiple sets of tensegrity structures. Viscoelastic properties were assigned to the continuum components. To corroborate the model, a simulation of atomic force microscopy indentation was performed and results showed a force/indentation simulation with the range of experimental results. A parametric analysis of both increasing membrane stiffness (thereby modelling membrane peroxidation with age) and decreasing density of cytoskeletal elements (thereby modelling reduced actin density with age) was performed. Comparing normal and aged cells under indentation predicts that aged cells have a lower membrane area subjected to high strain as compared with young cells, but the difference, surprisingly, is very small and may not be measurable experimentally. Ageing is predicted to have more significant effect on strain deep in the nucleus. These results show that computation of biophysical stimuli within cells are achievable with single-cell computational models; correspondence between computed and measured force/displacement behaviours provides a high-level validation of the model. Regarding the effect of ageing, the models suggest only small, although possibly physiologically significant, differences in internal biophysical stimuli between normal and aged cells.

1   Introduction

The mechanisms by which extracellular mechanical stimulation affects the differentiation of cells and ultimately cell fate is not yet well understood, despite its importance for tissue engineering and regenerative medicine (Ingber 2008; Wang et al. 2009). In particular, the role of ageing on the mechanoregulation of cell behaviour is a subject that has not yet been given very much consideration. Computational modelling can be used to explore potential mechanisms of cell response to mechanical stimuli. There have been several different approaches to modelling the complexity of cells:

(1)   The continuum approach described a single cell as a continuous cytoplasm covered within a cortical membrane (Evans and Yeung 1989; Karcher et al. 2003). Although, this approach has successfully demonstrated several cellular behaviours, it cannot describe the biophysical stimuli within cells because the cytoskeleton (CSK) network is not included in the cell models.

(2)   The tensegrity approach where the CSK is modelled as an interconnected network of cables and struts (Ingber 1997; Stamenovic and Coughlin 1999), with tensional cables representing actin filaments (AFs) and compressive struts representing microtubules. The stability of the structure is achieved by a balance of tension transmitted by cables and compression in the struts, which is induced by applying a pre-stress in the cables (Ingber 1993). This approach has been used to model many experimentally-observed aspects of cellular structural behaviour (Wang et al. 2001), such as prestress-induced stiffening and strain hardening (Coughlin and Stamenovic 1998; Wendling et al. 1999).

(3)   A hybrid approach that combines the continuum modelling with the tensegrity approach (De Santis et al. 2011; McGarry and Prendergast 2004; McGarry et al. 2005). These cell models consist of cellular components modelled as continua, including cytoplasm, nucleus, membrane, and a CSK, which was modelled as a tensegrity structure. More recently, nuclear tensegrity, with struts representing nuclear lamina and prestressed cables denoting chromatin, has been suggested (Ingber 2008) and researchers have demonstrated the importance of prestress in the nucleoskeleton (NSK) during cellular differentiation and development (Mazumder and Shivashankar 2010). With direct mechanical linkages between CSK and NSK confirmed [Wang et al. 2001; Dahl et al. 2010), the suggestion of an integrated CSK-NSK network, with both CSK and NSK modelled as tensegrities has been proposed (Dalby 2005; Ingber 2008).

It has been reported that the osteogenic and chondrogenic potential of mesenchymal stem cells (MSCs) reduces with the age of donor (Mueller and Glowacki 2001; Zheng et al. 2007). There are also reports showing that MSCs from aged donors display typical biomarkers of ageing. For example, McKayed et al. (2010) found that there is a decrease of , 35% in the expression of actin and integrin-a and an increase of 50% lipid peroxidation in MSCs of aged rats. Typically, in an aged cell membrane, the accumulation of lipid oxidation products in the cell membrane and growth of the domains with polysaturated fatty acids and cholesterol with age leads to an increase in averaged stiffness and viscosity of the lipid bilayer (Morris et al. 2004; Staroddubtseva 2011). Recently, Hale et al. (2011) have demonstrated that the amount of lipid peroxidation products found in cell membrane is approximately proportional to the membrane elasticity.

In this study, a finite element model of a cell was created using continuum modelling of the cell membrane, nucleus and cytoplasm, with multiple tensegrity structures included to represent both the CSK and the NSK. We aim to show that such a modelling approach can give force/ displacement predictions within the bounds of experimen- tal atomic force microscopy (AFM) indentation data. Although this would not fully validate the model, it would give confidence that it can be used to test the following hypotheses regarding the effect of changes in both membrane stiffness and cytoskeletal density (i.e. the structural changes observed due to ageing) on biophysical stimuli within the cell.

2 Methods

2.1 Geometry

The shape of the cell model was determined from experimental observations (Frisch and Thoumine 2002). The size of the cell model, including the proportion of nucleus, was based on confocal images of mesenchymal stem cells in our laboratory (Maguire et al. 2007). The CSK-NSK structure was modelled as follows: microtubules modelled as struts, AFs modelled as cables and intermediate filaments (IFs) were combined in the CSK as part of a pre-stressed tensegrity structure. Each tensegrity structure consists of six compression-bearing struts (two in each orthogonal direction) and twenty-four tensional cables representing the aggregate behaviour of microtubules and AF

4

bundles, respectively. Twelve common nodes were created at each end of the struts where four cables are connected, representing receptor sites where actin bundles cluster at adhesion complexes in adherent cells. To fit into a spread cell, the tensegrity structures that are derived from rounded configuration used by McGarry and Prendergast (2004) were incorporated. To mimic the complexity of the CSK three tensegrity structures were used (Figure 1 (a)). Three tensegrities were also used for the NSK, with struts representing nuclear lamina and chromatin modelled as cables (Figure 1 (b)). The nodes, where NSK contacts the nuclear surface, represent nuclear receptors spanning across the nuclear envelope that can receive mechanical signals from the CSK. Each nuclear receptor is connected to the corresponding cell receptor pointing in the same direction (Figure 2). These direct connections in the model represent the IFs. The cell model was developed using the finite element code ABAQUS/Standard version 6.8-1 (SIMULIA, RI, USA). Cytoplasm and nucleus were meshed with 4-node tetrahedral elements. Cell membrane and nuclear envelope were meshed with 3-node shell elements. A ''no-slip'' interaction condition was assumed at all nucleus–cytoplasm and cytoplasm–membrane interfaces (by employing the ''tie'' constraint in ABAQUS). Beam elements were used for struts and tension-only connecter elements were assigned to all the cables. A prestress that is equivalent to 2% of prestrain was assigned to all the cables that constitute tensegrity structures by giving a reference length to each of the connectors. A frictionless hard contact was used between the indenter surface and the cell membrane. Augmented Lagrange method was selected to model the contact by monitoring the gaps between pairs of nodes between the two surfaces.

2.2 Material modelling

Material properties for each of the cellular components are not known precisely for mesenchymal stem cells and can only be estimated from various sources. Viscoelastic properties were assigned to the cytoplasm, nucleus and membrane to incorporate time-dependant response to biophysical stimulation. A standard linear solid model, that consists of a spring k_1 paralleled with a series of another spring k_2 and a dashpot μ, was used to characterise the viscoelastic behaviour. The shear modulus $G(t)$, and the bulk modulus $K(t)$, at time t, are given as

$$G(t) = G(\infty)(1 - g^P (1 - e^{-\frac{t}{\tau}})) / (1 - g^P) \qquad Eqn.\ 1$$

$$K(t) = K(\infty)(1 - k^P (1 - e^{-\frac{t}{\tau}})) / (1 - k^P) \qquad Eqn.\ 2$$

5

where the parameters g^P, k^P and the relaxation time, τ are viscoelastic material constants, and $G(\infty)$ and $K(\infty)$ are the long-term shear and bulk moduli, respectively. Table 1 and Table 2 present the specific material properties for each cellular component used in this study.

Age-related changes regarding lipid peroxidation and expression of actin and integrin were interpreted and modelled by the following methods.

(1) In aged cells, both elastic modulus and apparent viscosity of the cell membrane were doubled relative to young cells to capture the effect of lipid peroxidation.

(2) The reduced amount of actin bundles and integrin receptors in aged cells was modelled by structural differences in CSK-NSK formation in our cell models. Specifically, two sets of CSK-NSK tensegrity combinations were used for the aged cells whereas three sets were used for the young cells.

2.3 Loading

Atomic force microscopy (AFM) is frequently used to investigate mechanical properties of biological cells (Radmacher et al. 1994). For example, Pillarisetti et al. (2011) measured non linear strain hardening in mouse embryonic cells using AFM indentation. In this study, a rigid conical indenter with a contact angle of 141 degrees was used to indent the cell model. A 3nN indenting force was applied to the indenter during each simulation in a force-control manner and the displacement at the indenter tip was computed with each increment. Two indenting rates, 1nN/s and 10nN/s, were investigated in this study. Simulations were carried out at two indenting positions on the cell membrane: at one of the receptor sites where the CSK contacts with cell membrane, and at the apex of the cell where is most distant from a receptor site. The stiffness of the cell model was calculated using a Hertz formula that relates the indenting force and indentation depth, which is expressed as

$$F = \frac{2E}{\pi \tan \alpha (1 - v^2)} \delta^2 \qquad Eqn.\ 3$$

where E is the stiffness of the cell, F is the reaction force at the indenter tip, α is a half of opening angle of the indenter tip, v is Poisson's ratio and δ is indentation depth.

3 Results

Using Equation (3), the elastic moduli of the cell models were calculated and averaged at 4.08 kPa at the apex and 5.87 kPa at the receptor site, indicating that indentation location has a great influence on the predicted cell stiffness. In comparison, age-related changes proposed in this study are not predicted to impact greatly on the stiffness of cells. A mere 5% increase in predicted stiffness is seen with the addition of age-related changes from 4.85 kPa for young cells to 5.09 kPa for aged cells. These predicted cell stiffness values were within the range of experimentally measured cell stiffness measured using AFM indentation (see Table 3).

A strain-hardening force–displacement behaviour was predicted for all AFM indentation simulations with the degrees of strain-hardening differing depending on indenta- tion site. The indenting position 2 at a receptor site versus at the apex distant from the receptor site – dominates the cells response to indenting force. An approximately 30% stiffer response is predicted when indenting at the receptor site, as compared with the case when indentation occurs at the apex of the cell. Although slight, age-related changes do affect the behaviour of cells under AFM indentation, indicating that cell stiffness changes with ageing (solid green curve vs. dashed brown curve; solid lime curve vs. dashed orange curve in Figure 3). An increase in the membrane stiffness stiffens cell's response to indenting force at both indentation locations, whereas a decrease in the complexity of CSK– NSK network increases the predicted cell stiffness at both indenting locations. The difference in cell stiffness caused by ageing is most apparent when indentation takes place at the apex of the cell (Figure 3). In the case of indenting at a receptor site where the CSK is in contact with cell membrane, a direct load transfer from indenter and CSK diminishes the impact of CSK complexity and membrane stiffness. In all cases, the indentation depth ranges from 13.7% to 23.4% of the original cell height, indicating that simulations are reliable and would return realistic results in a real experimental environment (Moeendarbary et al. 2013)

There is a striking difference in the pattern of stress inside a cell depending on indentation at the apex as compared with receptor site, compare Figure 4(a) with Figure 4(c) and compare Figure 4(b) with Figure 4(d). However, the difference due to ageing is not so visually obvious, compare Figure 4(a) with Figure 4(b) and compare Figure 4(c) with Figure 4(d). Apart from a stress concentration at the indenting location, the stress in the nucleus is higher than any other location in the cytoplasm: this is due to the IFs that transmit indenting force from cell membrane directly to the nucleus.

7

To quantify the strain difference in cell membrane when subjected to an indenting force, Von Mises strain was compared across all scenarios (Figures 4 and 5). Despite the difference made by age of the cell and indentation location, the total strained surface area decreases as strain range increases (Figure 5). Although almost no difference can be seen at mid-range, the differences are quite evident at low strain ranges. At high strain range, possibly at the interface between the cell and indenter, small differences in strained area can also be found.

A comparative study was carried out on the hydrostatic and deviatoric strain in the cell nucleus when undergoing indentation simulation at the cell apex (Figure 6). Although the young and aged cells exhibit no difference in terms of hydrostatic strain, deviatoric strain does show a slight difference, especially at low strain ranges. This suggests that the nuclei of the cells may be strained differently depending on the degree of ageing, with particular emphasis on the change in shape rather than volume.

4   Discussion

We tested the hypothesis that there is a change in the biophysical stimuli inside a cell as a consequence of the changes in membrane stiffness and cytoskeletal element density that occur with age. This hypothesis has been corroborated because the analysis predicted that strains, both in cell membrane and nucleus, differ with age-related changes known to occur in cellular components; however, the changes are not as high as might be anticipated, except for the differences of the area under low strains (Figure 5).

This study exemplifies the potential utility of a hybrid continuum-tensegrity representation of a cell. A particular strength of this approach is the ability to separate the potential load transfer mechanisms within a cell due to externally applied stimuli. Nevertheless, even this relatively complex tensegrity representation of the CSK –NSK does not capture the true complexity and dynamic behaviour observed in real cells and should therefore be considered as a tool to understand the aggregate behaviour of cytoskeletal mechanics at instants of time rather than an accurate representation of CSK – NSK structure and mechanics under all circumstances. Furthermore, because of the nature of a passive model, this approach does not capture any active behaviour that a cell would exhibit under mechanical loading.

Cellular finite element modelling provides insight into the cell biomechanics, which could not

be achieved experimentally. The idea of using multiple units of tensegrity structures presented in this paper enabled us to investigate the influence of ageing on cells' behaviour by capturing aged-related structural changes in CSK. It also provides us a closer-to-reality view on cell modelling, as compared with single tensegrity approach (Ingber 1993). By integrating the CSK and NSK networks in a cell model, the presentation of direct mechanical linkages from cell membrane to nucleus through AFs and IFs (Wang and Stamenovic 2000, 2002), then reaching deep into the nucleus via Linker of NSK and CSK (LINC)-complex that were discovered recently (Wang et al. 2009; Dahl et al. 2010) allows us to explore the possibilities of how external mechanical signal affects nuclear biophysical stimuli. The difference found in CSK complexity with regard to donor age alters the force-transfer pattern within the cells and ultimately differentiate the biophysical stimuli received by the nuclei (see Figure 6).

AFM is frequently used to investigate the mechanical properties of biological cells (Radmacher et al. 1994). For example, Ng et al. (2007) measured nonlinear strain hardening in bovine chondrocytes using AFM indentation. During AFM indentation simulation, common mechanical nonlinear responses are present in all force displacement curves. These strain-hardening behaviours are consistent with previous experimental data in the literature (Figure 3). There are several sources contributing to this typical strain- hardening behaviour. First of all, it is most obvious that this nonlinearity is because of the viscoelastic nature of the cytoplasm, nucleus and membrane. Second, tensegrity structures contribute to this nonlinear behaviour; it has been demonstrated by Stamenovic et al. (1996) that six-strut tensegrity structures of such a type used in this study have strain-hardening and nonlinear characteristics. This contribution can be further confirmed by a computational study done by McGarry and Prendergast (2004), in which a strain-hardening effect was achieved, even without viscoelastic properties used in any cellular component. Also, during the indentation process, the area of contact surface between the indenter and the cell membrane increases as the indenter travels deeper into the cell. An increasing resistance to the indenter induced by this enlarging contact area decelerates the indenter and nonlinearity is achieved as a result.

Our results suggest that indentation location greatly affects the measured cell stiffness using AFM (Figures 3 and 4). Although this is in agreement with the experimental investigations in the literature (Ohashi et al. 2002), a much stiffened behaviour is predicted in the case of indenting at a receptor site, as compared with experimental observations. In theory, this is due to the fact that the indenting force is directly transferred to the CSK, which is a much stiffer structure. In practice, such a

difference will not be evident due to slippage between the indenter tip and cell membrane, with an exception that coatings are applied to the indenter tip to specifically target receptors on the membrane by chemical binding.

Most interestingly, we found age-related changes that we assigned to the cell model spell influences on the predicted cell stiffness. Specifically, the aged cell is slightly stiffer than the young cell at both indenting locations. This is largely due to the stiffer material properties used for cell membrane that is caused by products of higher level of lipid peroxidation in aged cells. In this study, we doubled the membrane stiffness for the aged cells by assuming a proportional relationship between the amount of lipid peroxidation product and membrane stiffness (Hale et al. 2011). However, as much as 450% increase in the elasticity of membrane is suggested when doubling the amount of lipid peroxidation products according to Ajmani et al. (2000). This would further increase the difference in predicted cell stiffness at both indentation locations (Figure 3). Differences caused by ageing can also be seen deep in the nucleus. Despite the almost identical hydrostatic strains found in the nuclei of both young and aged cells, the deviatoric strain in the nucleus differs between young and aged cells, which is due to the difference in the density of cytoskeletal filament and the number of focal adhesion sites which transmit extracellular mechanical stimuli into the cell. This could be important, as it has been demonstrated that these direct linkages transmit mechanical signals many times faster than biochemical responses (Wang et al. 2009).

The predicted results on cell membrane strain during AFM indentation simulations suggest that young cells tend to have a greater membrane area under high strain (Figure 5). If this is true, it would lead to opening of more mechanosensitive stretch-activated ion channels (Charras and Horton 2002a, 2002b). It has been shown that openings of mechanosensitive channel could give rise to whole cell cytosolic calcium responses, thereby reinforcing the putative role of mechanosensitive channels as the first step in the transduction of external physiological mechanical stimuli into whole cell responses (Charras et al. 2004). The differences in the number of receptor sites and the complexity of the CSK – NSK network that mechanically connect the extracellular matrix to the nucleus, between the young and the aged cells, could result in a difference in stimulation patterning in the nucleus, as shown in Figure 6. Nuclear strain has been suggested to influence higher-order chromatin organisation, thereby restricting or promoting the accessibility of transcription factors or other regulatory factors to specific gene sequences, which could similarly influence gene transcription (Stein et al. 2007).

5 Conclusion

A 3D finite element model of a single cell with a complex CSK –NSK network was developed. AFM indentation tests were simulated on the cell model with age-related changes applied. Our results show that indenting location dominates cells behaviour under indentation loading environment. In comparison, the effect of age-related changes on the predicted cell stiffness is minor. However, differences are found in both membrane strain and nuclear strain, despite the small change in predicted cell stiffness due to ageing, indicating that there is a change in the biophysical stimuli inside a cell as a consequence of ageing. In this study, only two configurations of CSK – NSK structures were included. The authors recommend future researchers to comprehensively look into CSK – NSK complexity in order to capture the mechanical and structural changes occurring with ageing.

6 Acknowledgements

7   References

Azeloglu U, Bhattacharya J, Costa KD. 2008. Atomic force microscope elastography reveals phenotypic differences in alveolar cell stiffness. J Appl Physiol. 105(2):652– 661.

Bertaud J, Qin Z, Buehler MJ. 2010. Intermediate filament-deficient cells are mechanically softer at large deformation: a multi-scale simulation study. Acta Biomater. 6(7):2457-2466.

Charras GT, Horton MA. 2002a. Single cell mechanotransduction and its modulation analyzed by atomic force microscope indentation. Biophys J. 82(6):2970-2981.

Charras GT, Horton MA. 2002b. Determination of cellular strains by combined atomic force microscopy and finite element modeling. Biophys J. 83(2):858-879.

Charras GT, Williams BA, Sims SM, Horton MA. 2004. Estimating the Sensitivity of Mechanosensitive Ion Channels to Membrane Strain and Tension. Biophys J. 87(4):2870-2884.

Collinsworth AM, Zhang S, Kraus WE, Truskey GA. 2002. Apparent elastic modulus and hysteresis of skeletal muscle cells throughout differentiation. Am J Physiol–Cell Ph. 283(4):1219-1227.

Coughlin MF, Stamenovic D. 1998. A tensegrity model of the cytoskeleton in spread and round cells. J Biomech Eng. 120(6):770-777.

Dahl KN, Booth-Gauthier EA, Ladoux B. 2010. In the middle of it all: mutual mechanical regulation between the nucleus and the cytoskeleton. J Biomech. 43(1):2-8.

Dahl KN, Kahn SM, Wilson KL, Discher DE. 2004. The nuclear envelope lamina network has elasticity and a compressibility limit suggestive of a molecular shock absorber. J Cell Sci. 117(20):4779-4786.

Dalby MJ. 2005. Topographically induced direct cell mechanotransduction. Med Eng Phys. 27(9):730-742.

De Santis G, Lennon AB, Boschetti F, Verhegghe B, Verdonck P, Prendergast PJ. 2011. How can cells sense the elasticity of a substrate? An analysis using a cell tensegrity model. Eur Cell Mater. 22:202-213.

Deguchi S, Ohashi T, Sato M. 2005. Evaluation of tension in actin bundle of endothelial cells based on preexisting strain and tensile properties measurements. Mol Cell Biomech. 2(3):125-133.

Evans E, Yeung A. 1989. Apparent viscosity and cortical tension of blood granulocytes determined by micropipet aspiration. Biophys J. 56(1):151-160.

Frisch T, Thoumine O. 2002. Predicting the kinetics of cell spreading. J Biomech. 35(8):1137-1141.

Gittes F, Mickey B, Nettleton J, Howard J. 1993. Flexural rigidity of microtubules and actin filaments measured from thermal fluctuations in shape. J Cell Biol. 120(4):923-934.

Guilak F, Tedrow JR, Burgkart R. 2000. Viscoelastic properties of the cell nucleus. Biochem Bioph Res Co. 269(3):781-786.

Ingber DE. 1997. Tensegrity: the architectural basis of cellular mechanotransduction. Annu Rev Physiol. 59:575-599.

Ingber DE. 2008. Tensegrity-based mechanosensing from macro to micro. Prog Biophys Mol Biol. 97(2-3):163-179.

Ingber DE. 1993. Cellular tensegrity: defining new rules of biological design that govern the cytoskeleton. J Cell Sci. 104(3):613 -627.

Kamm RD, McVittie AK, Bathe M. 2000. On the Roleof Continuum Models in Mechanobiology. ASME International Congress - Mechanics in Biology. 242:1-9.

Karcher H, Lammerding J, Huang H, Lee RT, Kamm RD, Kaazempur-Mofrad MR. 2003. A three-dimensional viscoelastic model for cell deformation with experimental verification. Biophys J. 85(5):3336-3349.

Kelly GM, Kilpatrick JI, van Es MH, Weafer PP, Prendergast PJ, Jarvis SP. 2011. Bone cell elasticity and morphology changes during the cell cycle. J Biomech. 44(8):1484-1490.

Maguire P, Kilpatrick JI, Kelly GM, Prendergast PJ, Campbell VA, O'Connell BC, Jarvis SP. 2007. Direct mechanical measurement of geodesic structures in rat mesenchymal stem cells. HFSP J. 1(3):181-191.

Mazumder A, Shivashankar GV. 2010. Emergence of a prestressed eukaryotic nucleus during cellular differentiation and development. J Roy Soc Inter. 7(3):321-330.

McGarry JG, Prendergast PJ. 2004. A three-dimensional finite element model of an adherent eukaryotic cell. Eur Cell Mater. 7:27-33.

McGarry JG, Klein-Nulend J, Mullender MG, Prendergast PJ. 2005. A comparison of strain and fluid shear stress in stimulating bone cell responses--a computational and experimental study. FASEB J. 19(3):482-484.

McKayed KK, Campbell VA, Prendergast PJ. 2010. The influence of age on mesenchymal stem cell mechanoresponsiveness to tensile strain. Paper presented at: ESB 2010. Proceedings of the 17th Congress of European Society of Biomechanics, July 5–8, University of Edinburgh, UK.

Morris R, Cox H, Mombelli E, Quinn PJ. 2004. Rafts, little caves and large potholes: how lipid structure interacts with membrane proteins to create functionally diverse membrane environments. SubCell Biochem. 37:335-118.

Mueller SM, Glowacki J. 2001. Age-related decline in the osteogenic potential of human bone marrow cells cultured in three-dimensional collagen sponges. J Cell Biochem .82(4):583-590.

Ohashi T, Ishii Y, Ishikawa Y, Matsumoto T, Sato M. 2002. Experimental and numerical analyses of local mechanical properties measured by atomic force microscopy for sheared endothelial cells. BioMed Mater Eng. 12(3):319-327.

Pillarisetti A, Desai JP, Ladjal H, Schiffmacher A, Ferreira A, Keefer CL. 2011. Mechanical phenotyping of mouse embryonic stem cells: increase in stiffness with differentiation. Cell Reprog. 13(4):371-380.

Radmacher M, Cleveland JP, Fritz M, Hansma HG, Hansma PK. 1994. Mapping interaction forces with the atomic force microscope. Biophys J. 66(6):2159-2165.

Roduit C, van der Goot FG, De Los Rios P, Yersin A, Steiner P, Dietler G, Catsicas S, Lafont F, Kasas S. 2008. Elastic membrane heterogeneity of living cells revealed by stiff nanoscale membrane domains. Biophys J. 94(4):1521-1532.

Shin D, Athanasiou K. 1999. Cytoindentation for obtaining cell biomechanical properties. J Orthop Res. 17:880-890.

Smith SB, Cui Y, Bustamante C. 1996. Overstretching B-DNA: the elastic response of individual double-stranded and single-stranded DNA molecules. Sci NY. 271(5250):795-799.

Stamenovic D, Coughlin MF. 1999. The role of prestress and architecture of the cytoskeleton and deformability of cytoskeletal filaments in mechanics of adherent cells: a quantitative analysis. J Theor Biol. 201(1):63-74.

Stamenovic D, Fredberg JJ, Wang N, Butler JP, Ingber DE. 1996. A Microstructural Approach to Cytoskeletal Mechanics based on Tensegrity. J Theor Biol. 181(2):125-136.

Starodubtseva MN. 2011. Mechanical properties of cells and ageing. Ageing Res Rev. 10(1):16-25.

Stein GS, Lian JB, van Wijnen AJ, Stein JL, Javed A, Montecino M, Choi J, Vradii D, Zaidi SK, Pratap J, Young D. 2007. Organization of transcriptional regulatory machinery in nuclear microenvironments: implications for biological control and cancer. Adv Enzyme Regul. 47:242-250.

Stolzing A, Scutt A. 2006. Age-related impairment of mesenchymal progenitor cell function. Aging Cell. 5(3):213-224.

Suresh S, Spatz J, Mills JP, Micoulet MD, Lim CT, Beil M, Seufferlein T. 2005. Connections between single-cell biomechanics and human disease states: gastrointestinal cancer and malaria. Acta Biomaterialia. 1(1):15-30.

Wang N, Stamenovic D. 2000. Contribution of intermediate filaments to cell stiffness, stiffening, and growth. Am J Physiol Cell Physiol. 279(1):188-194.

Wang N, Stamenovic D. 2002. Mechanics of vimentin intermediate filaments. J Muscle Res Cell M. 23(5-6):535-540.

Wang N, Naruse K, Stamenovic D, Fredberg JJ, Mijailovich SM, Tolic-Norrelykke IM, Polte T, Mannix R, Ingber DE. 2001. Mechanical behavior in living cells consistent with the tensegrity model. Proceedings of the National Academy of Sciences; USA. 98(14):7765-7770.

Wang N, Tytell JD, Ingber DE. 2009. Mechanotransduction at a distance: mechanically coupling the extracellular matrix with the nucleus. Nat Rev Mol Cell Biol. 10(1):75-82.

Waugh RE, Agre P. 1988. Reductions of erythrocyte membrane viscoelastic coefficients reflect spectrin deficiencies in hereditary spherocytosis. J Clin Invest. 81(1):133-141.

Wendling S, Oddou C, Isabey D. 1999. Stiffening response of a cellular tensegrity model. J Theor Biol. 196(3):309-325.

Wu M, Fannin J, Rice KM, Wang B, Blough ER. 2011. Effect of aging on cellular mechanotransduction. Ageing Res Rev. 10(1):1-15.

Zheng H, Martin JA, Duwayri Y, Falcon G, Buckwalter JA. 2007. Impact of aging on rat bone marrow-derived stem cell chondrogenesis. J Gerontol Biol Sci Med Sci. 62(2):136-148.

Table 1. Viscoelastic properties of cellular components

	k_1 (Pa)	k_2 (Pa)	μ (kPa.s)	Piosson's ratio
Cytoplasm*[#]	50	100	5	0.37
Nucleus*[#]	200	400	10	0.37
Membrane[¶§]	720	280	25	0.3

*Shin and Athanasiou, 2001; [#]Guilak et al. 2000; [¶]Waugh & Agre 1988; [§]Kamm et al. 2000.

Table 2. Elastic and geometric properties of cellular components

	Elastic modulus (Pa)	Poisson's ratio	Diameter (nm)
Microtubules*	$1.2×10^9$	0.3	12
AF bundles[#]	$0.34×10^6$	0.3	250
Ifs[¶]	$7.6×10^6$	0.3	10
Lamina[§]	$1.4×10^6$	0.3	10
Chromatin[ς]	$244×10^6$	0.3	1.2

*Gittes et al. 1993, [#]Deguchi et al. 2005, [¶]Bertaud et al. 2010, [§]Dahl et al. 2004, [ς]Smith et al. 1996.

Table 3. Experimentally measured cell stiffness using AFM from previous studies

Cell type	Measured stiffness (kPa)
mESC*	1.49±0.09
Fibroblast[#]	6.00±2.30
Myoblast[¶]	11.50±1.30
Osteoblast[§]	5.20±0.60 (S phase)
	2.30±3.30 (G1 phase)

*Pillarisetti et al. 2011; [#]Azeloglu et al. 2008; [¶]Collinsworth et al. 2002; [§]Kelly et al. 2011.
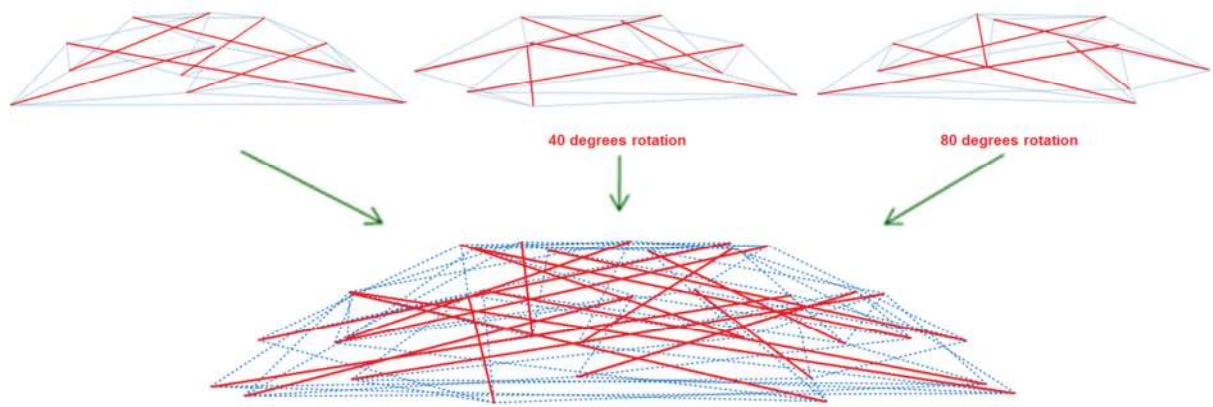
Figure 1 (A) The formation of cytoskeletal network. It is formed by 3 sets of 6-strut flattened tensegrity structures, with the identical second and third set rotated along y-axis by 40 and 80 degrees clockwise, respectively, with struts (red lines) representing microtubules and cables (blue dotted lines) representing actin bundles.
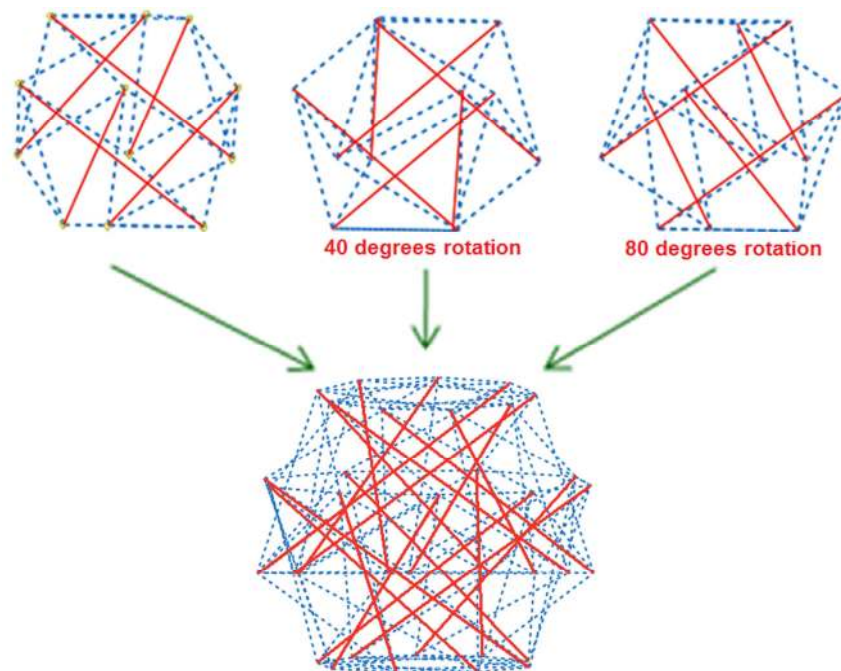

Figure 1 (B) The formation of nucleoskeletal network. The same method shown in Figure 1 (A) applies to 3 sets round-configuration tensegrity structures, with nuclear lamina and chromatin modelled by struts and cables, respectively.
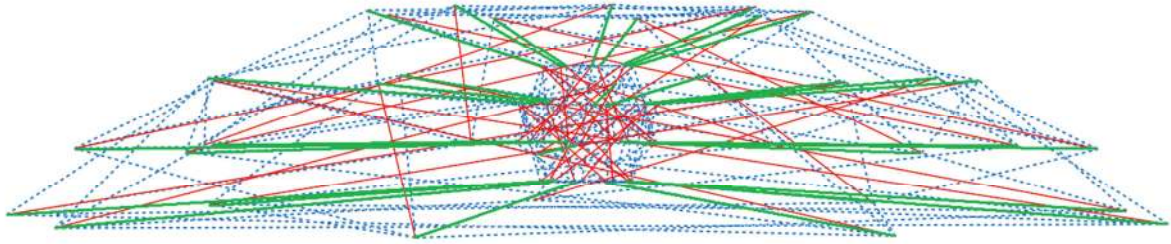
Figure 2. NSK (Figure 1 (A)) was then placed at the centre of the CSK (Figure 1 (B)) and the two structures are connected by direct linkages representing IFs (shown in green lines).
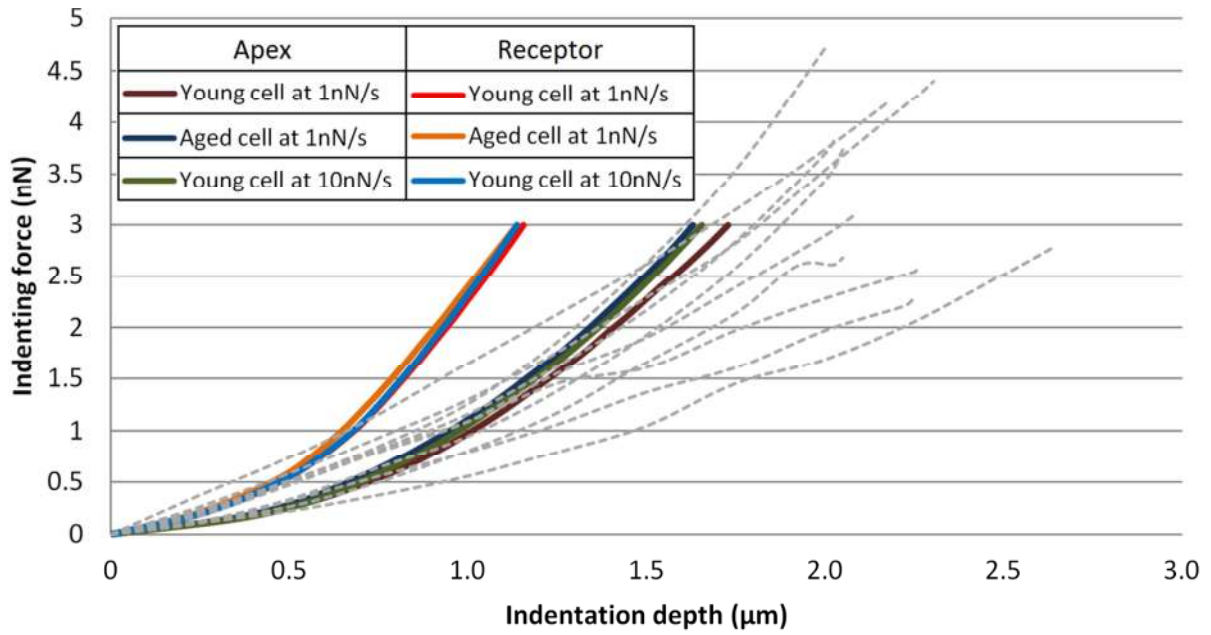
Figure 3. Force-displacement curves from indentation at two different indenting locations (apex and a receptor site) at two different loading rates (1nN/s and 10nN/s) for young and aged cells. The data for indenting at apex at a loading rate of 10nN/s are not shown for the sake of clarity. The experimental data are taken from a study measuring the stiffness of mouse embryonic stem cells using AFM indentation carried out by Pillarisetti et al. (2011).
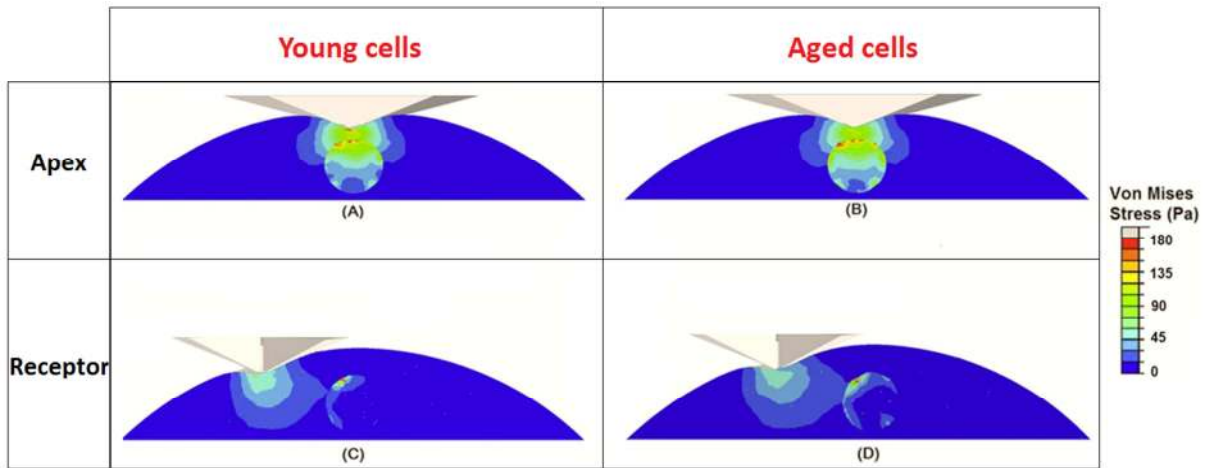
Figure 4. Contour plots of Von Mises stress during indentation simulation with different indenting locations, at apex (A, B) and a receptor site (C, D) of young cells (A, C) and aged cells (B, D). Cut-views are shown for visual comparison of Von Mises stress inside the cells.
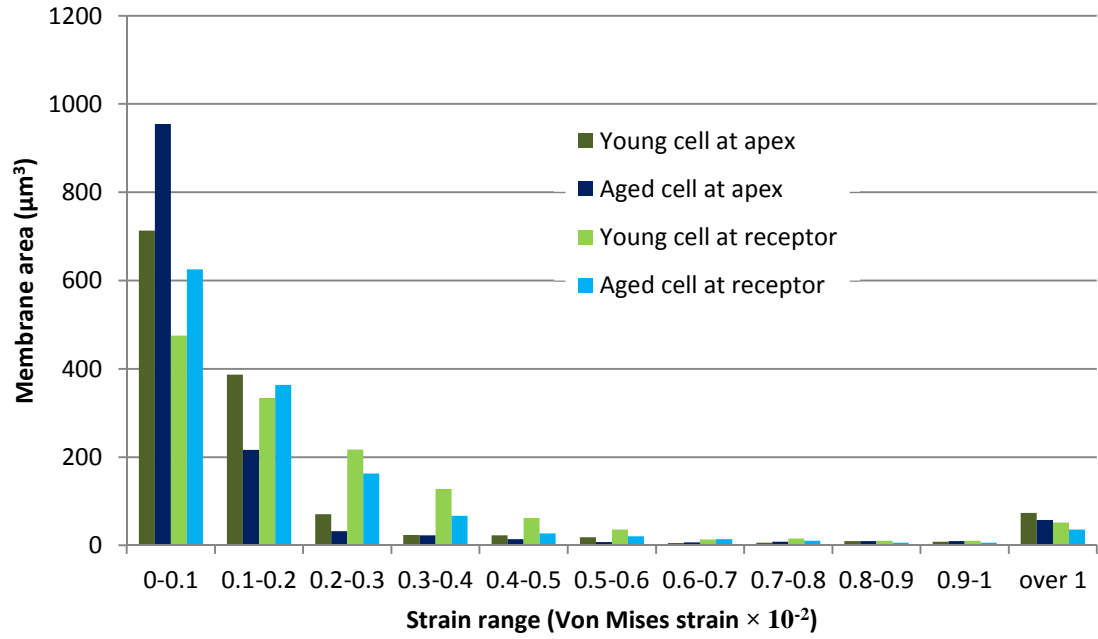
Figure 5. Area of membrane apposed to a given strain range. Aged cells have smaller membrane area under high strain and correspondingly have greater membrane area under low strain, than young cells subjected to indentation.
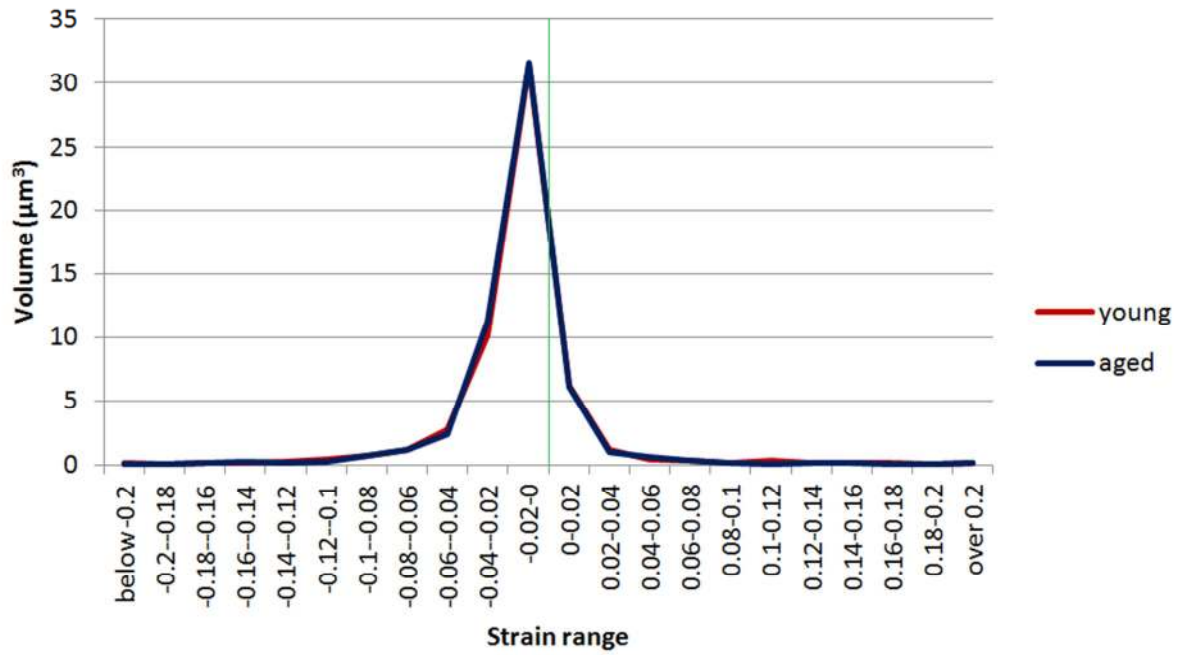
Figure 6 (A). Volume of nucleus exposed to a given strain range (hydrostatic strain). The slim green indicates zero strain location. Little difference can be seen between the aged and young cells.
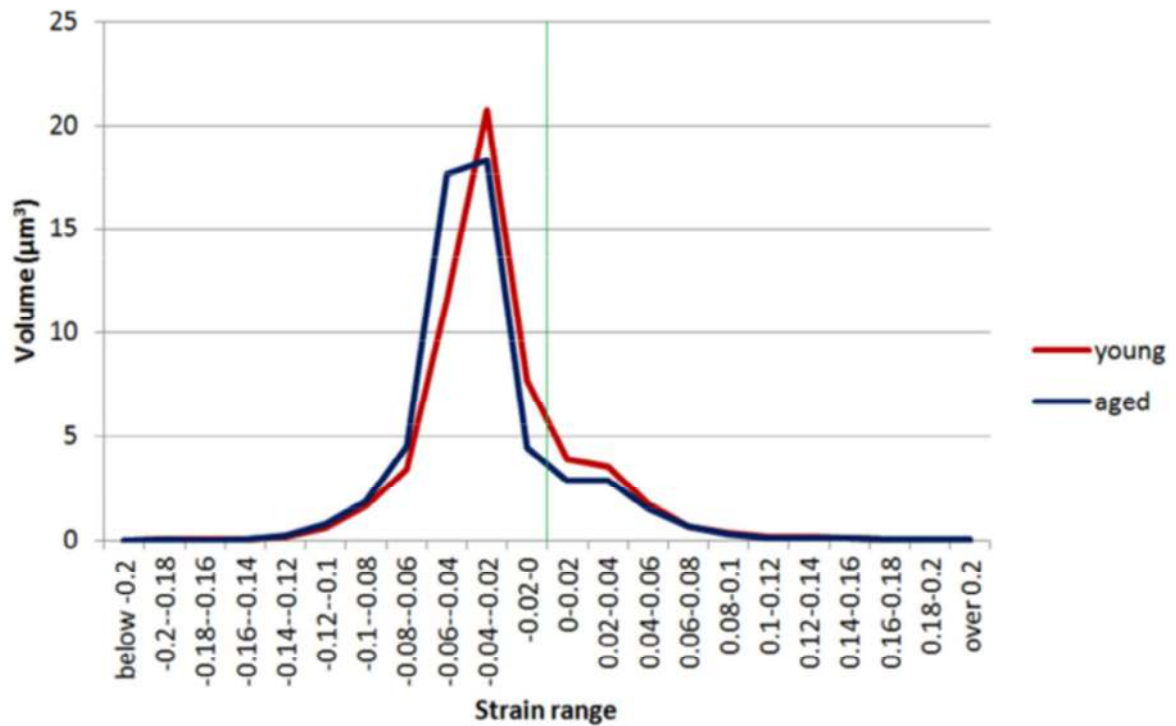

Figure 6 (B). Volume of nucleus apposed to a given strain range (deviatoric strain). The slim green indicates zero strain location. Differences are seen between aged and young cells at mid-low strain ranges, particularly in the negative region.